Supplementary Materials

Trimetallic strategy towards $Zn^{II}_4Dy^{III}_2Cr^{III}_2$ and $Zn^{II}_4Dy^{III}_2Co^{III}_2$ single-ion magnets

Kong-Qiu Hu,† Xiang Jiang,† Shu-Qi Wu,† Cai-Ming Liu,‡ Ai-Li Cui,† Hui-Zhong Kou*†

† Department of Chemistry, Tsinghua University, Beijing 100084, P. R. China. ‡ Beijing National Laboratory for Molecular Sciences, Center for Molecular Science, Institute of Chemistry, Chinese Academy of Sciences, Beijing 100190, P. R. China

Physical measurements

IR spectra were recorded on a Nicolet Magna-IR 750 spectrometer in the 4000-450 cm^{-1} region. Elemental analyses (C, H, N) were performed on an Elementar Vario MICRO CUBE analyzer. Metallic elemental analyses were carried out on an inductively coupled plasma atomic emission spectrometer. Temperature- and field-dependent magnetic susceptibility measurements were carried out on a Quantum Design SQUID magnetometer. The experimental susceptibilities were corrected for the diamagnetism of the constituent atoms (Pascal's Tables).

Single crystal X-ray data were collected on a Rigaku Saturn724+ CCD diffractometer for complexes **1** and **2**. The structures were solved by direct method (SHELXS-97) and refined by full-matrix least-squares (SHELXL-2014) on F^2. Anisotropic thermal parameters were used for the non-hydrogen atoms and isotropic parameters for the hydrogen atoms. Hydrogen atoms were added geometrically and refined using a riding model. Because of the weak crystal diffraction of complexes **1** and **2**, some solvents

DMF/CH_3CN/H_2O molecules experience serious disorder, and cannot be completely found from the difference Fourier map. Therefore the SQUEEZE function of PLATON was applied.

Synthesis of $\{[Zn(Me_2valpn)]_2Dy(H_2O)Co(CN)_6\}_2\cdot 15H_2O\cdot 2DMF\cdot 5CH_3CN$ ***(1).*** $Zn(Me_2valpn)$ (93 mg, 0.2 mmol) and $Dy(NO_3)_3\cdot 6H_2O$ (46mg, 0.1 mmol) were mixed in MeCN (10 mL), and $K_3[Co(CN)_6]$ (33 mg, 0.1 mmol) in water (5 mL) was then added into the above solution. The resultant solution was stirred for 5 minutes, and was filtered. To the filtrate, DMF (1 mL) was added. The solution was slowly evaporated at room temperature for 2 hrs to afford colorless block single crystals. IR (KBr, cm^{-1}): 2127,2162 (C≡N). Anal. Calcd for complex **1** ($C_{112}H_{159}Dy_2Co_2N_{27}Zn_4O_{35}$): C 42.73, H 5.09, N 12.01, Co 3.74, Zn 8.31, Dy 10.32. Measured: C 42.69, H 5.39, N 11.74, Co 3.8, Zn 8.6, Dy 10.1.

Synthesis of $\{[Zn(Me_2valpn)]_2Dy(H_2O)Cr(CN)_6\}_2\cdot 7H_2O\cdot 4DMF$ ***(2).*** $Zn(Me_2valpn)$ (93 mg, 0.2 mmol) and $Dy(NO_3)_3\cdot 6H_2O$ (46mg, 0.1 mmol) were mixed in MeCN (10 mL), and $K_3[Cr(CN)_6]$ (32 mg, 0.1 mmol) in water (5 mL) was then added into the above solution. The resultant solution was stirred for 5 minutes, and was filtered. To the filtrate, DMF (1 mL) was added. The solution was slowly evaporated at room temperature for 2 hrs to afford buff block single crystals. IR (KBr, cm^{-1}): 2108, 2168 (C≡N). Anal. Calcd for complex **2** ($C_{108}H_{140}Dy_2Cr_2N_{24}Zn_4O_{29}$): C 44.29, H 4.82, N 11.48, Cr 3.55, Zn 8.93, Dy 11.10. Measured: C 44.62, H 4.93, N 11.64, Cr 3.6, Zn 8.6, Dy 11.0.

Table S1. X-ray crystallographic parameters for complexes **1** and **2**

complex	**1**	**2**
formula	$C_{112}H_{159}Dy_2Co_2N_{27}Zn_4O_{35}$	$C_{108}H_{140}Dy_2Cr_2N_{24}Zn_4O_{29}$
Fw	3148.00	2928.92
T/K	163	163
crystal system	Monoclinic	Monoclinic
space group	*P*2(1)/*c*	*P*2(1)/*c*
a/Å	20.089(3)	16.929(3)
b/Å	15.835(2)	22.842(5)
c/Å	28.012(3)	20.172(4)
β/º	128.896(7)	105.86(3)
V /Å^3	6935(2)	7503(3)
Z	2	2
ρ_{calcd}/g cm^{-3}	1.507	1.296
μ(MoKa)/ mm^{-1}	2.057	1.816
F(000)	3212	2976
Ref [I >2σ]	12951	8868
GOF	1.065	0.980
R1[I > 2σ(I)][a]	0.0479	0.1000
wR2 (all data)[b]	0.1403	0.2924

[a] $R1=\Sigma \; // \; F_o| - |F_c \; ||/ \Sigma|F_o|$. [b] $wR2=\{\Sigma[w(F_o^2 - F_c^2)^2]/\Sigma[w(F_o^2)^2]\}^{1/2}$

Table S2 Selected bond distances (Å) and bond angles (°) for complex **1**

Dy(1)–O(6)	2.323(3)	Zn(2)–O(6)	2.071(3)
Dy(1)–O(1W)	2.316(3)	Zn(1)–N(6)	2.018(4)
Dy(1)–O(2)	2.334(3)	Zn(1)–O(1)	2.028(3)
Dy(1)–O(5)	2.376(3)	Zn(1)–N(4)	2.042(4)
Dy(1)–O(1)	2.393(3)	Zn(1)–N(3)	2.074(4)
Dy(1)–O(7)	2.478(3)	Zn(1)–O(2)	2.087(3)
Dy(1)–O(3)	2.485(3)	Co(1A)–C(6)	1.789(5)
Dy(1)–O(4)	2.535(3)	Co(1A)–C(10A)	1.905(10)
Dy(1)–O(8)	2.554(3)	Co(1A)–C(9)	1.812(5)
Zn(2)–N(9)	2.006(4)	Co(1A)–C(11A)	1.932(11)
Zn(2)–N(2)	2.050(4)	Co(1A)–C(8B)	1.946(12)
Zn(2)–N(1)	2.067(4)	Co(1A)–C(7A)	1.903(10)
Zn(2)–O(5)	2.058(3)	Co(1B)–C(6)	1.999(6)
Co(1B)–C8A)	1.877(14)	Co(1B)–C(9)	1.974(6)
Co(1B)–C(11B)	1.878(14)	Co(1B)–C(10B)	1.881(13)
Co(1B)–C7B)	1.941(16)		
Co(1A)–C(6)–N(6)	173.3(5)	N(6)–C(6)–Co(1B)	170.5(5)
Co(1A)–C(9)–N(9)	171.8(5)	N(10B)–C(10B)–Co(1B)	179.2(16)
Co(1A)–C(8B)–N(8B)	178.0(10)	N(8A)–C(8A)–Co(1B)	176.9(15)
Co(1A)–C(7A)–N(7A)	178(3)	N(7B)–C(7B)–Co(1B)	175(4)
Co(1A)–C(10A)–N(10A)	176.1(10)	Zn(2)–O(5)–Dy(1)	107.46(11)
Co(1A)–C(11A)–N(11A)	178.6(12)	Zn(1)–O(2)–Dy(1)	108.05(12)
N(11B)–C(11B)–Co(1B)	177.3(18)	Zn(2)–O(6)–Dy(1)	108.97(12)
N(9)–C(9)–Co(1B)	171.8(5)	Zn(1)–O(1)–Dy(1)	107.91(12)
C(6)–N(6)–Zn(1)	155.8(4)	C(9)–N(9)–Zn(2)#1	160.2(4)

#1: 1-x, 2-y, 2-z

Table S3 Selected bond distances (Å) and bond angles (°) for complex **2**

Dy(1)–O(5)	2.356(6)	Zn(2)–N(7)	2.133(11)
Dy(1)–O(1)	2.364(7)	Zn(1)–O(6)	2.039(6)
Dy(1)–O(1W)	2.416(7)	Zn(1)–N(9)	2.066(9)
Dy(1)–O(2)	2.433(7)	Zn(1)–N(10)	2.066(9)
Dy(1)–O(6)	2.467(6)	Zn(1)–N(1)	2.073(8)
Dy(1)–O(8)	2.526(6)	Zn(1)–O(5)	2.122(6)
Dy(1)–O(4)	2.536(6)	Cr(1)–C(4)	2.071(7)
Dy(1)–O(7)	2.571(6)	Cr(1)–C(1)	2.086(10)
Dy(1)–O(3)	2.595(6)	Cr(1)–C(5)	2.095(9)
Zn(2)–N(8)	2.054(10)	Cr(1)–C(6)	2.096(10)
Zn(2)–N(3)	2.069(9)	Cr(1)–C(3)	2.111(10)
Zn(2)–O(2)	2.084(7)	Cr(1)–C(2)	2.131(11)
Zn(2)–O(1)	2.095(8)		
Cr(1)–C(1)–N(1)	172.9(10)	Cr(1)–C(6)–N(6)	175.5(12)
Cr(1)–C(2)–N(2)	172.9(8)	Zn(2)–O(1)–Dy(1)	109.1(3)
Cr(1)–C(3)–N(3)	172.6(9)	Zn(2)–O(2)–Dy(1)	107.0(3)
Cr(1)–C(4)–N(4)	169.0(13)	Zn(1)–O(5)–Dy(1)	108.5(2)
Cr(1)–C(5)–N(5)	177.0(10)	Zn(1)–O(6)–Dy(1)	107.3(2)

Table S4. Continuous Shape Measures calculation for the Dy(III) ions in complexes **1-2**

Nine-coordination

Complex **1**, Dy structures

Structure [ML9]	EP-9	OPY-9	HBPY-9	JTC-9	JCCU-9	CCU-9	JCSAPR-9	**CSAPR-9**	JTCTPR-9	TCTPR-9	JTDIC-9	HH-9	**MFF-9**
ABOXIY	34.512	21.991	17.249	14.843	8.405	7.387	3.826	**2.483**	5.402	2.572	10.197	7.195	**2.266**

Nine-coordination

Complex **2**, Dy structures

Structure [ML9]	EP-9	OPY-9	HBPY-9	JTC-9	JCCU-9	CCU-9	JCSAPR-9	**CSAPR-9**	JTCTPR-9	TCTPR-9	JTDIC-9	HH-9	**MFF-9**
ABOXIY	34.297	21.691	17.461	14.330	8.812	7.656	3.577	**2.218**	5.072	2.403	9.592	7.642	**2.105**

EP-9	1	D9h	Enneagon
OPY-9	2	C8v	Octagonal pyramid
HBPY-9	3	D7h	Heptagonal bipyramid
JTC-9	4	C3v	Johnson triangular cupola J3
JCCU-9	5	C4v	Capped cube J8
CCU-9	6	C4v	Spherical-relaxed capped cube
JCSAPR-9	7	C4v	Capped square antiprism J10
CSAPR-9	8	C4v	Spherical capped square antiprism
JTCTPR-9	9	D3h	Tricapped trigonal prism J51
TCTPR-9	10	D3h	Spherical tricapped trigonal prism
JTDIC-9	11	C3v	Tridiminished icosahedron J63
HH-9	12	C2v	Hula-hoop
MFF-9	13	Cs	Muffin

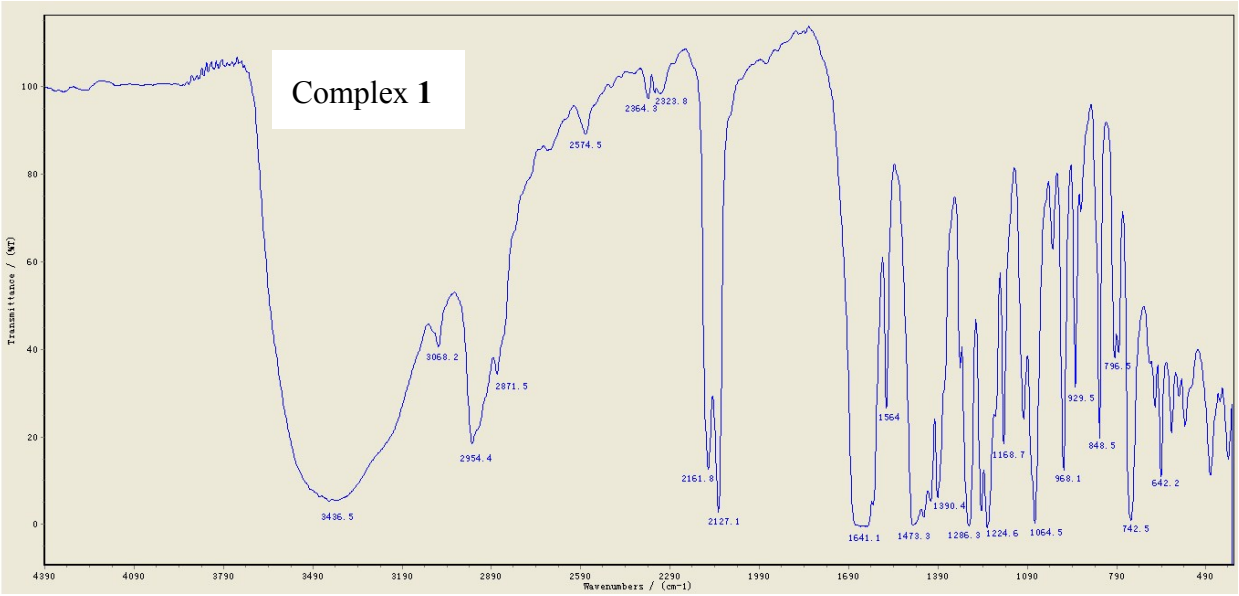

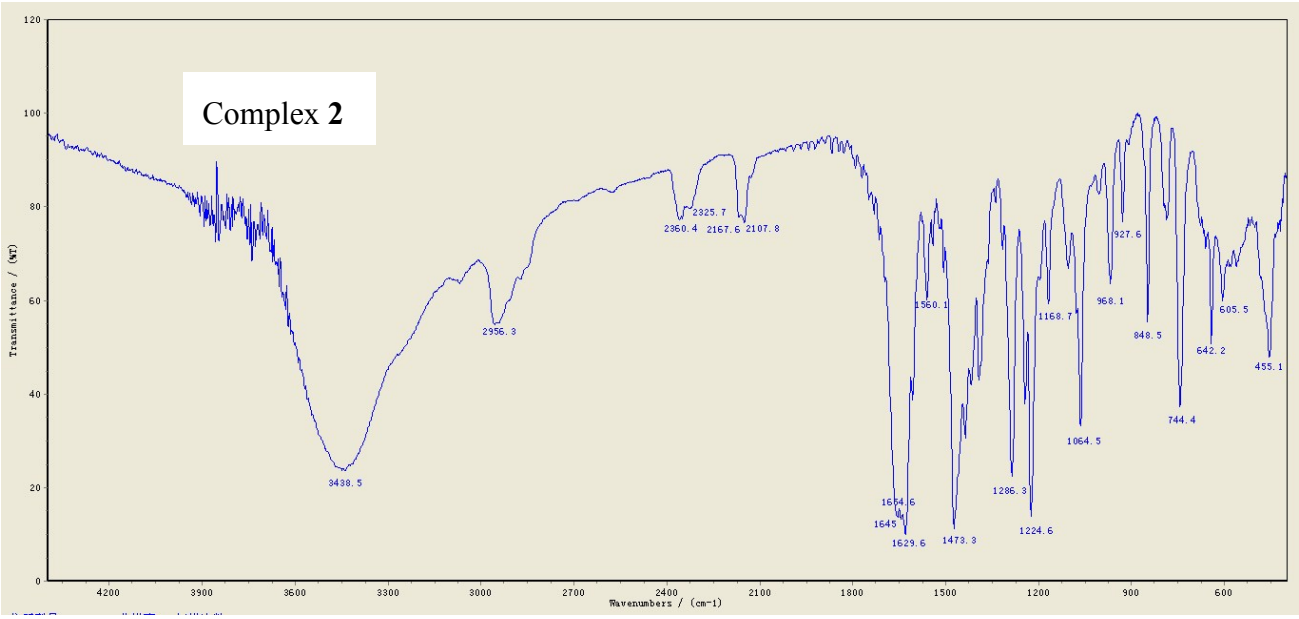

Fig. S1. IR spectra of complexes **1-2**.

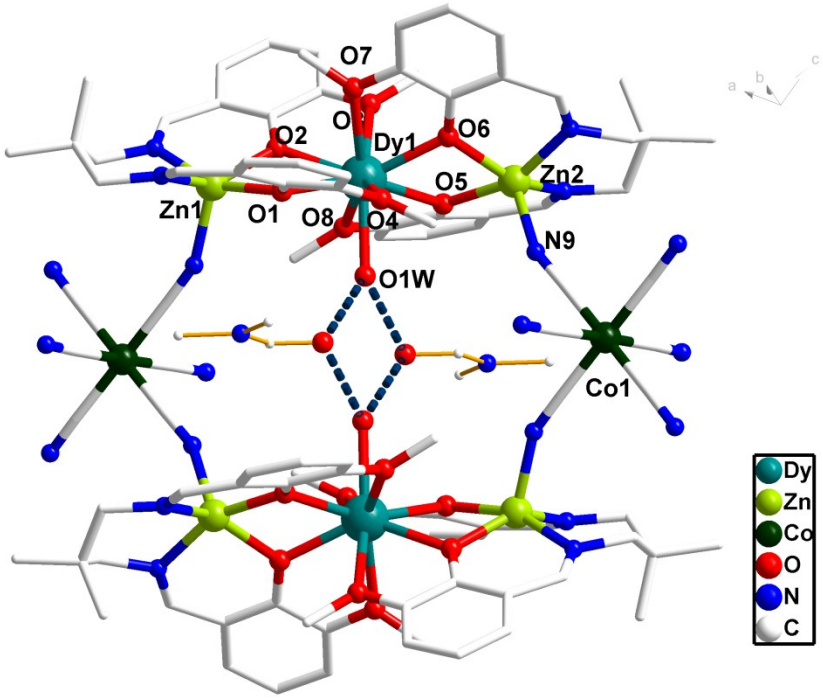

Fig. S2. The hydrogen bonding in complex **1**.

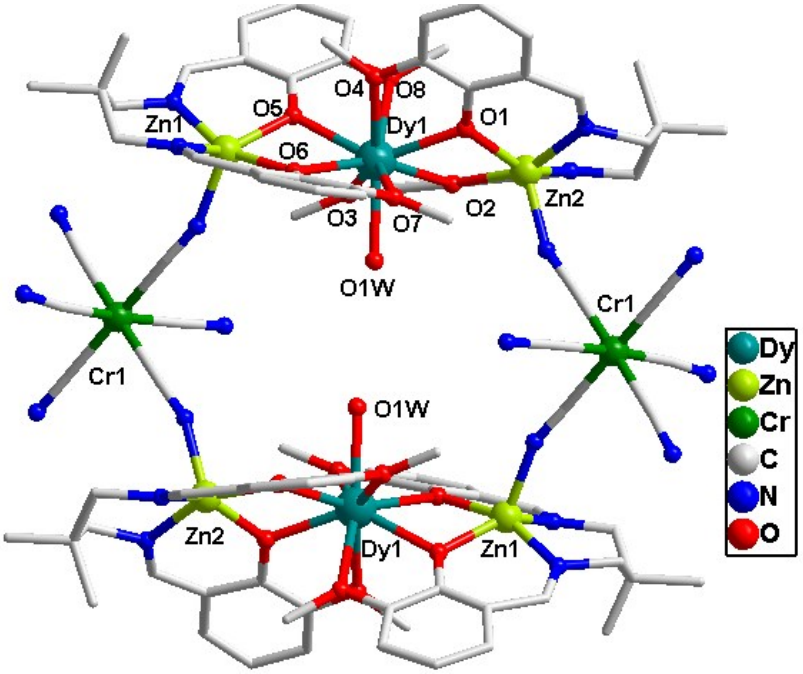

Fig. S3. The octanuclear cyclic structure of complex **2**.

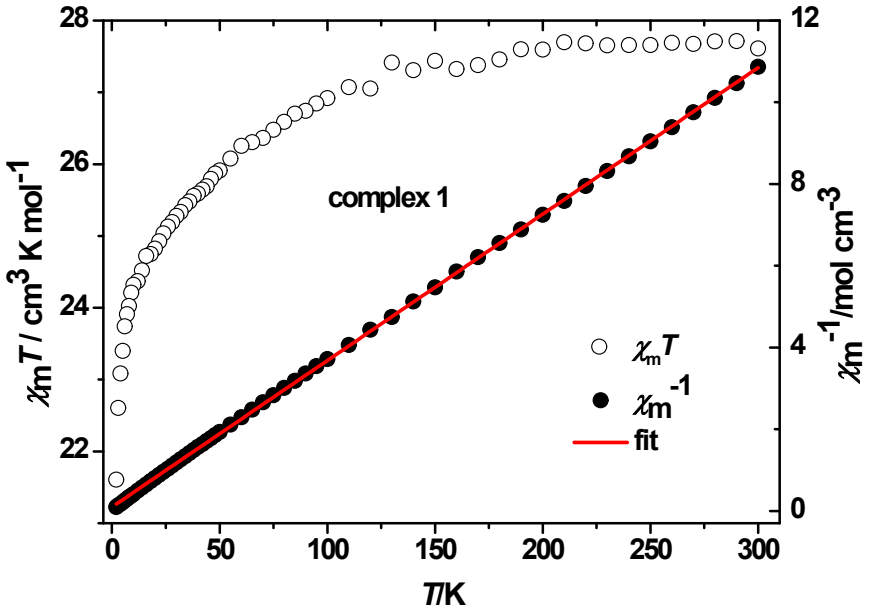

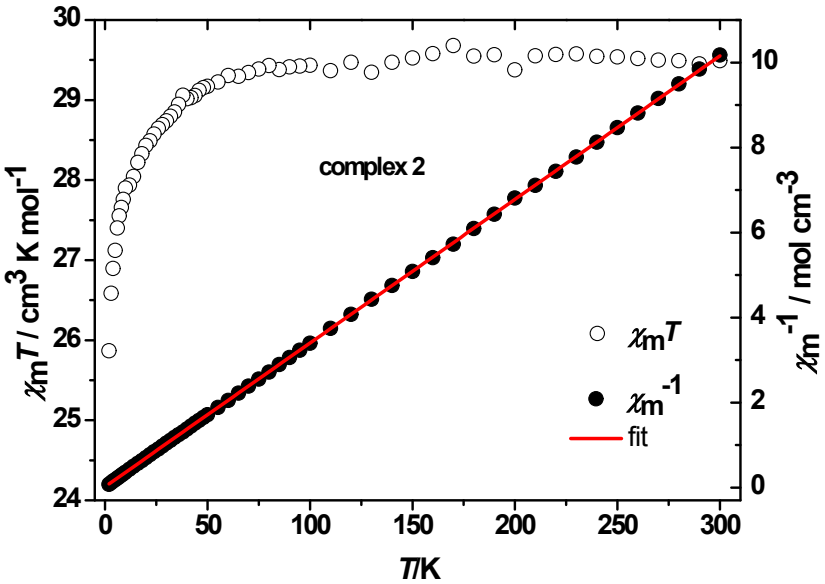

Fig. S4. Temperature dependence of $\chi_m T$ for complexes **1-2**.

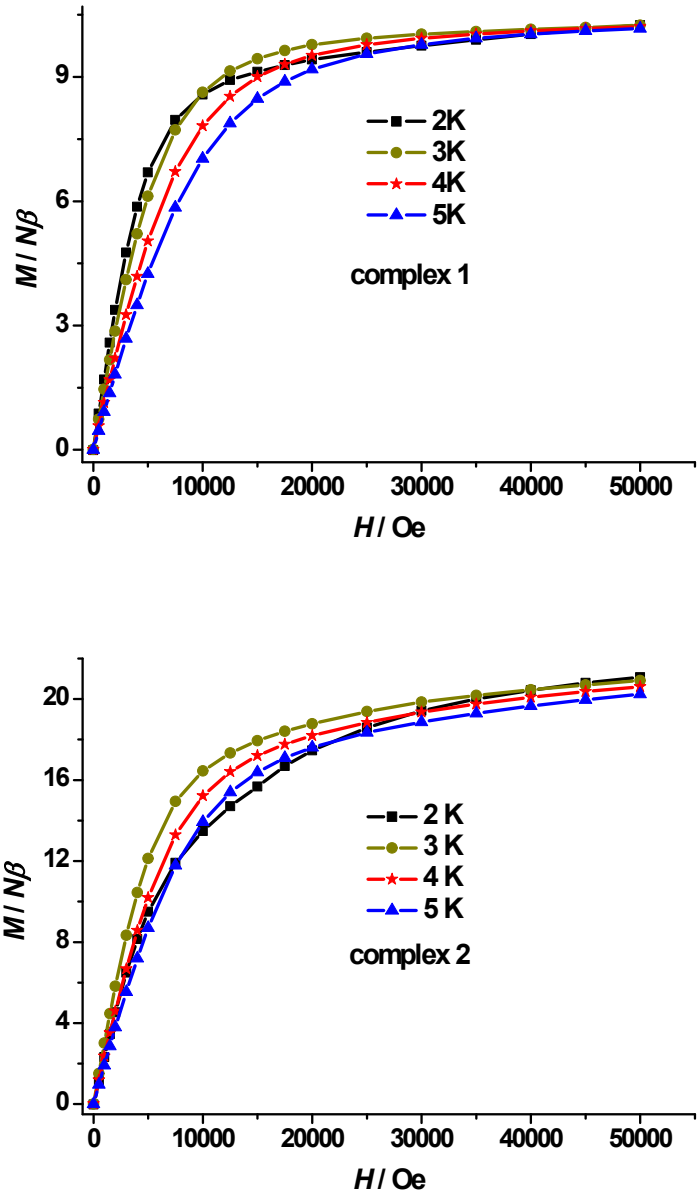

Fig. S5. Temperature dependence of the magnetic susceptibilities at 2-5 K for complexes **1-2**.

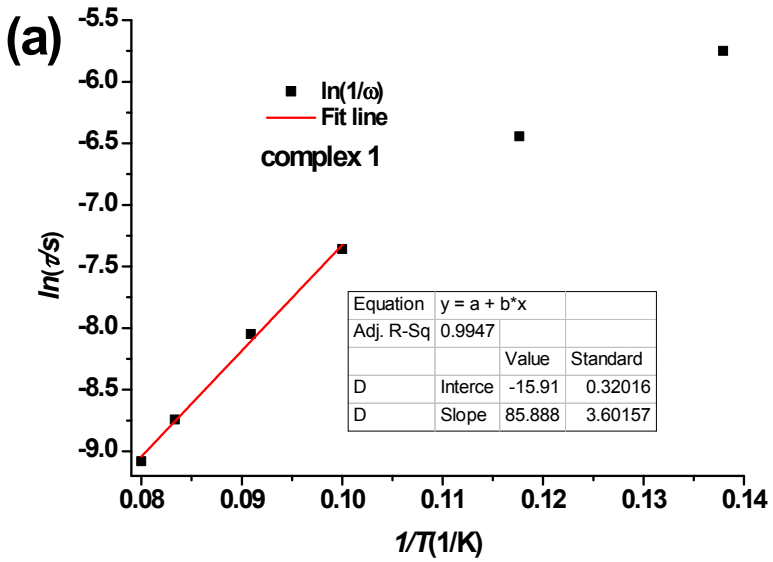

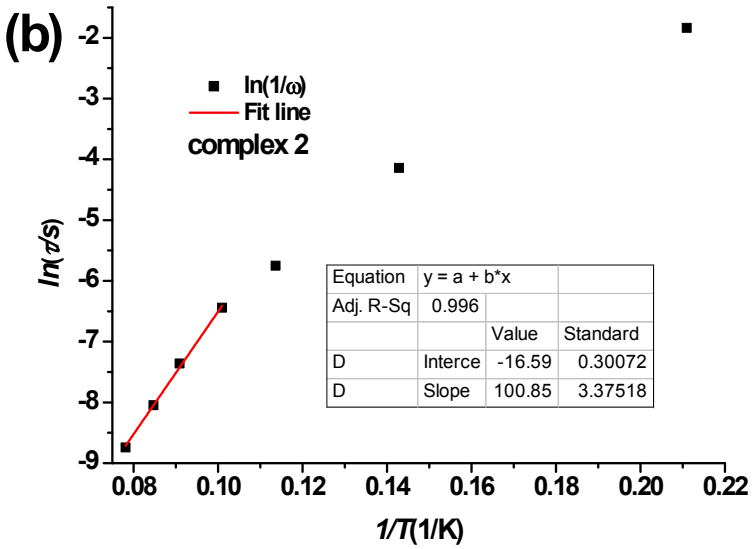

Fig. S6. The ln(τ) vs. T^{-1} plots based on the Arrhenius relationship for complexes **1** (a) and **2** (b).

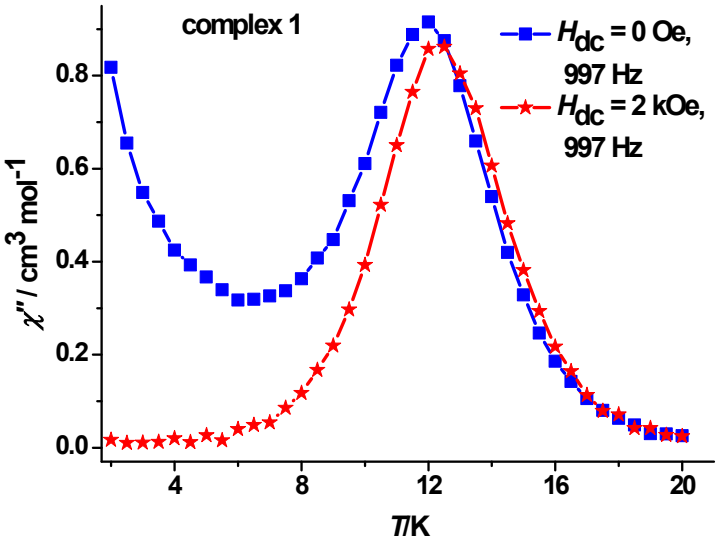

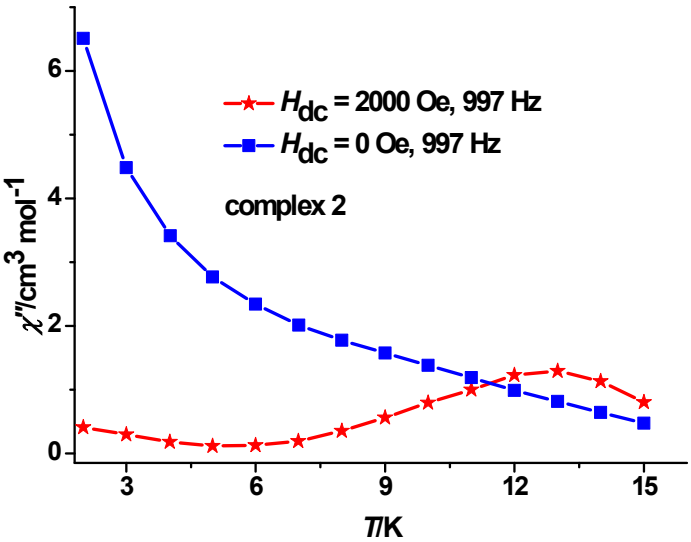

Fig. S7. The out-of-phase (χ_m'') ac magnetic susceptibilities for complexes **1-2** in 997 Hz under zero and 2 kOe dc field.

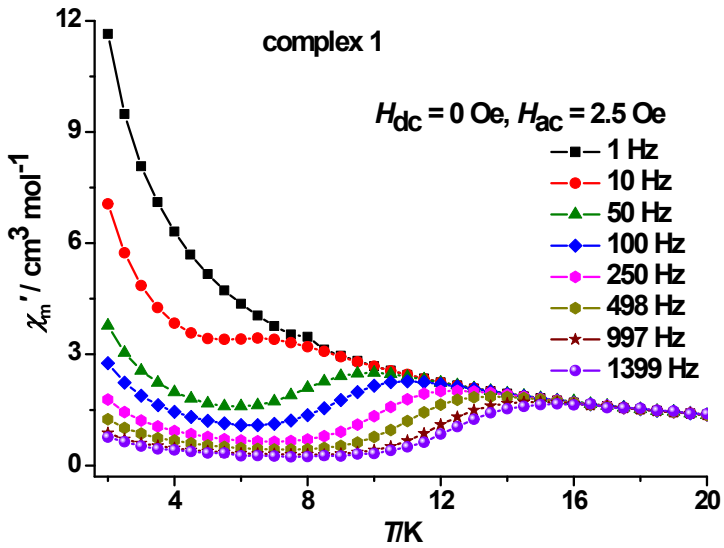

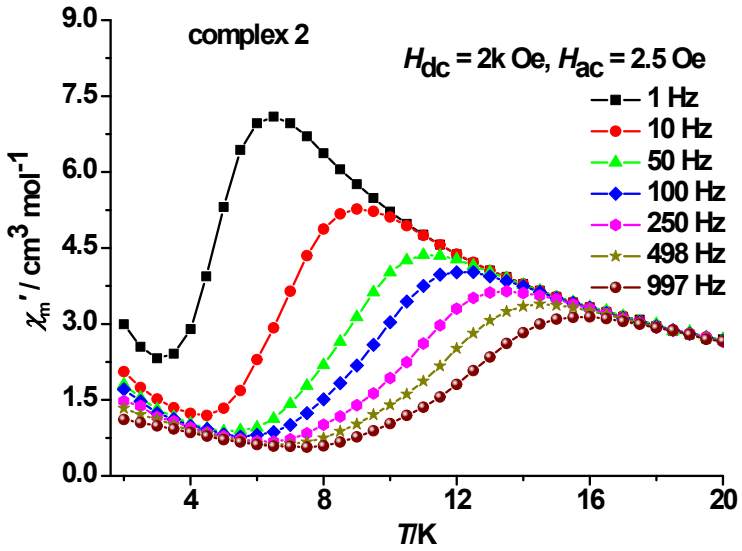

Fig. S8. The in-phase (χ_m') ac magnetic susceptibilities for complexes **1-2** under zero and 2 kOe dc field.

Fit of Cole-Cole plots. The derivation of Debye model mentioned in the text is applied and displayed here:

$$\chi'_M = \chi_1 + (\chi_T - \chi_S)\left(\frac{\beta(1+(\omega\tau_1)^{1-\alpha_1})\sin\left(\frac{\pi}{2}\alpha_1\right)}{1+2(\omega\tau_1)^{1-\alpha_1}\sin\left(\frac{\pi}{2}\alpha_1\right)+(\omega\tau_1)^{2(1-\alpha_1)}}+\frac{(1-\beta)(1+(\omega\tau_2)^{1-\alpha_2})\sin\left(\frac{\pi}{2}\alpha_2\right)}{1+2(\omega\tau_2)^{1-\alpha_2}\sin\left(\frac{\pi}{2}\alpha_2\right)+(\omega\tau_2)^{2(1-\alpha_2)}}\right)$$

$$\chi''_M = (\chi_T - \chi_S)\left(\frac{\beta((\omega\tau_1)^{1-\alpha_1})\cos\left(\frac{\pi}{2}\alpha_1\right)}{1+2(\omega\tau_1)^{1-\alpha_1}\sin\left(\frac{\pi}{2}\alpha_1\right)+(\omega\tau_1)^{2(1-\alpha_1)}}+\frac{(1-\beta)((\omega\tau_2)^{1-\alpha_2})\cos\left(\frac{\pi}{2}\alpha_2\right)}{1+2(\omega\tau_2)^{1-\alpha_2}\sin\left(\frac{\pi}{2}\alpha_2\right)+(\omega\tau_2)^{2(1-\alpha_2)}}\right)$$

Table S5. Parameters in double magnetic relaxations for complex **1**

T / K	α		τ		χ		β
	α_1	α_2	τ_1	τ_2	χ_T	χ_S	
2	0.14	0.42	0.187	0.028	12.59	0.16	0.38
4	0.41	0.11	0.0249	0.164	6.706	0.11	0.58
6	0.31	0.028	0.0121	0.0672	4.44	0.41	0.13
7	0.029	0.258	0.037	7.4×10^{-3}	3.81	0.12	0.61
8	0.21	0.024	4.8×10^{-3}	0.021	3.34	0.12	0.35
9	0.17	0.018	3.3×10^{-3}	0.011	2.98	0.10	0.37
10	4.6×10^{-3}	0.103	6.5×10^{-3}	2.3×10^{-3}	2.69	0.11	0.55
11	1.5×10^{-14}	0.079	3.6×10^{-3}	1.4×10^{-3}	2.45	0.11	0.43
12	0.046	2.69×10^{-14}	0.046	2.7×10^{-14}	2.25	2.8×10^{-18}	0.72

Table S6. Parameters in double magnetic relaxations for complex **2**

T / K	α		τ		χ		β
	α_1	α_2	τ_1	τ_2	χ_T	χ_S	
2	0.24	0.42	0.00142	72.29	26.05	0.6341	0.0438
4	0.38	0.21	1.2×10^{-4}	3.61	11.93	1.4×10^{-15}	0.0845
6	0.21	0.31	0.328	3.4×10^{-5}	8.71	3.6×10^{-13}	0.93
8	0.32	0.09	0.0129	0.0642	6.51	0.39	0.34
10	0.373	1.2×10^{-13}	0.0038	0.014	5.35	0.24	0.59
12	0.064	0.13	0.0034	7.7×10^{-4}	4.39	0.63	0.59

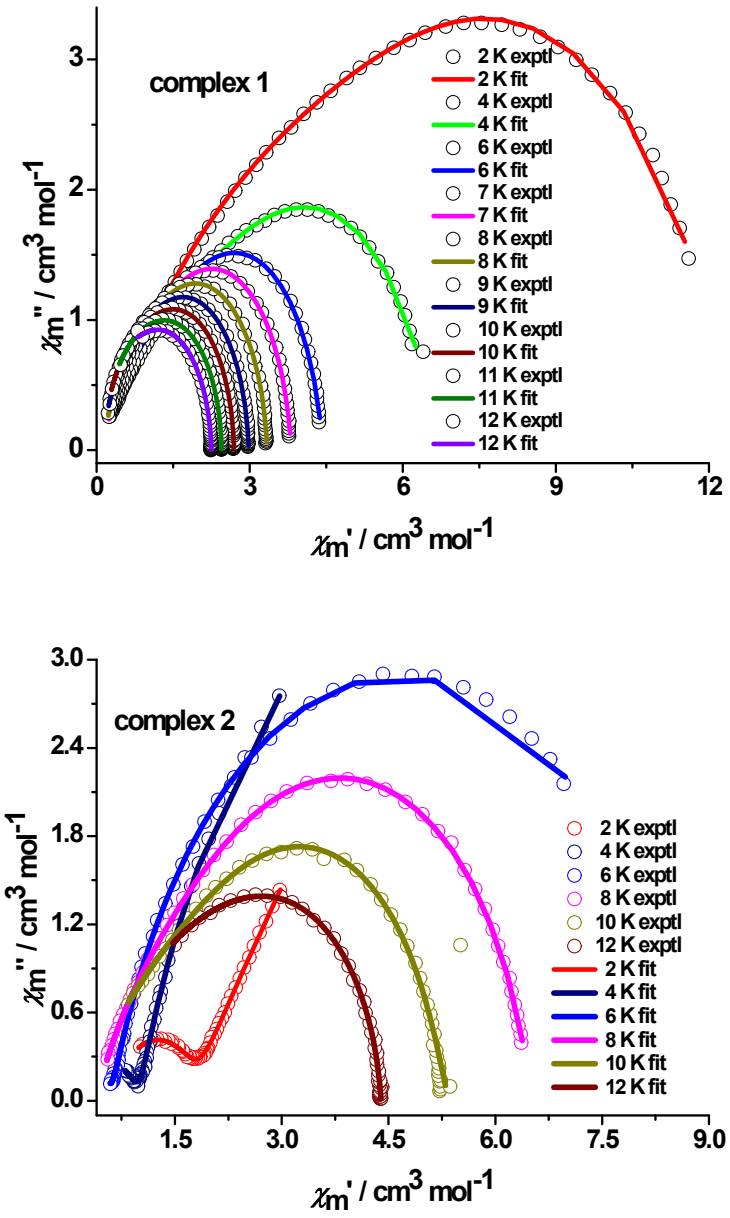

Fig. S9. Cole-Cole plots of complexes **1** (H_{dc} = 0 Oe and H_{ac} = 2.5 Oe) and **2** (H_{dc} = 2 kOe and H_{ac} = 2.5 Oe). The solid lines represent the best fit results.

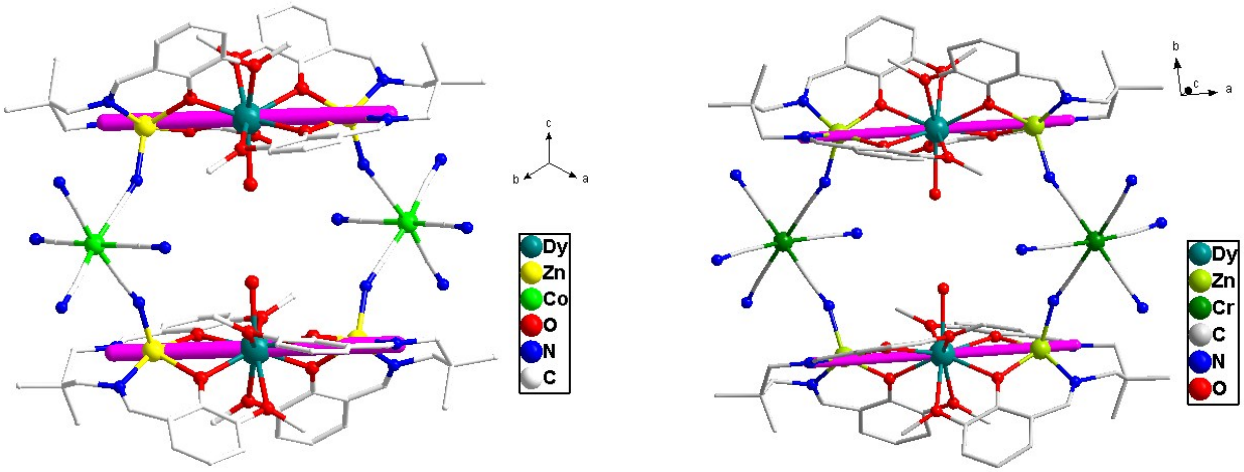

Fig. S10. Direction of the anisotropic axis of Dy(III) ions in complexes **1** (Left) and **2** (Right).

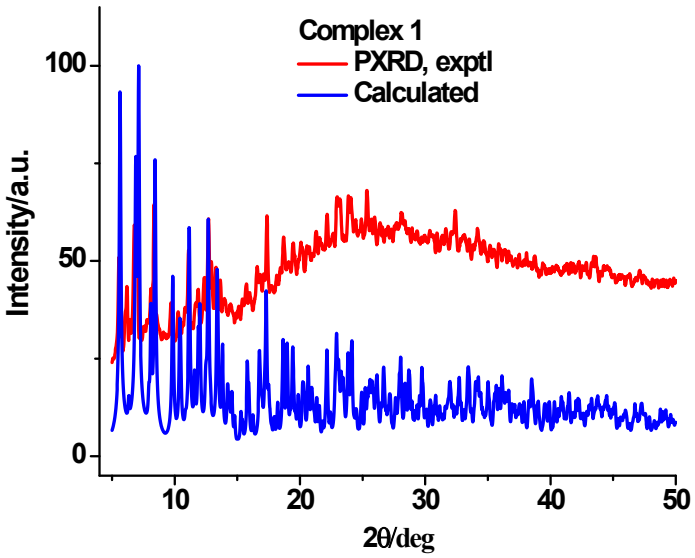

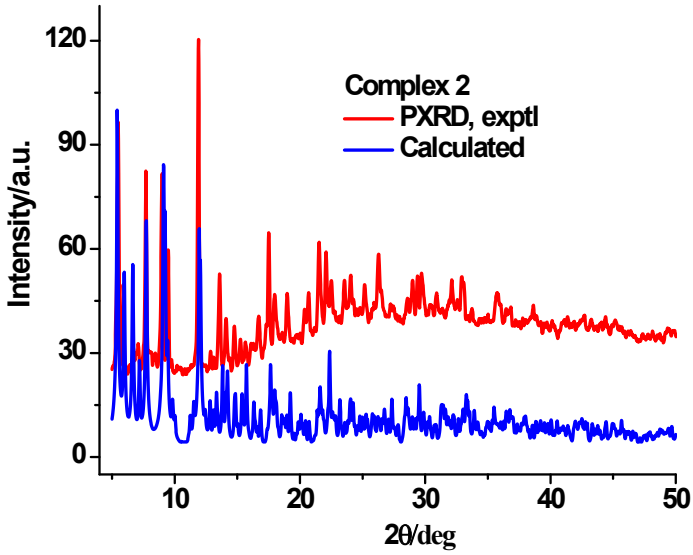

Fig. S11. Powder XRD patterns of complexes **1** and **2**.